ORGANOMETALLICS

pubs.acs.org/Organometallics

Article

Moving on from Silicon to the Heavier Tetrels: Germyl- and Stannyl-Substituted Phosphole Derivatives

Fabian Roesler, Máté Kovács, Clemens Bruhn, Zsolt Kelemen,* and Rudolf Pietschnig*

Cite This: *Organometallics* 2023, 42, 793−802

Read Online

ACCESS | Metrics & More | Article Recommendations | Supporting Information

ABSTRACT: Germyl- and stannyl-substituted phospholes have been prepared and isolated. The increased reactivity of the tetrel carbon bond requires increased effort in purification by initial transformation to the chalcogen derivatives and subsequent reduction to the phosphole after subsequent to chromatographic purification for the germanium derivative. The photophysical properties of the germyl phosphole are comparable to that of its silyl analogue, whereas the stannyl phospholes turned out to be nonluminescent. All isolated compounds have been characterized by NMR spectroscopy, mass spectrometry, and elemental analysis. Furthermore, single-crystal X-ray diffraction and density functional theory (DFT) calculations have been performed on selected compounds.

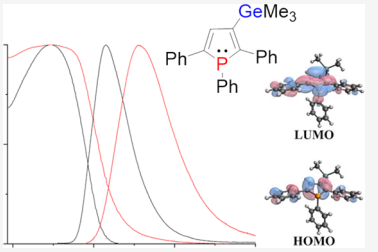

INTRODUCTION

Phosphorus-containing heterocycles are an exceptionally versatile class of compounds with unique and attractive properties.[1−7] A prominent example is the respective unsaturated five-membered heterocycles, known as phospholes.[8] These have emerged as attractive π-conjugated materials and luminophores with remarkable photophysical features highlighting their potential for future applications.[9−13] From a synthetic point of view, modification at the phosphorus atom *via* reduction or formal oxidation is quite common in phospholes.[14] However, selective functionalization at the carbon backbone of the phosphole ring is relatively rare in contrast to their nitrogen analogues, the highly aromatic pyrroles.[15] A few years ago, we developed synthetic access to phospholes carrying one or two silyl units in the β-position of the heterocycle in high yields.[16,17] Initially, this approach focused mainly on trimethylsilyl units (TMS) but later was expanded to functional silyl groups allowing for immobilization of the phosphole to oxide-based surfaces *via* grafting.[9,18] The silyl units may be used for tuning the steric and electronic properties of the phosphole and desilylation reactions have been explored for further derivatization of the heterocyclic ring system.[9,17−19] These findings inspired us to explore the possibility of attaching the heavier congeners as germyl and stannyl units at the phosphole system *via* the route previously established for β-silyl phospholes.

While a few stannyl phosphole derivatives have been already reported by Matano (type **VI** and **VII**, Figure 1) and Mathey (type **IV** and **V**), in fact, only a single report for a germanium-containing phosphole derivative has been previously published which does not involve a classical germyl unit (type **V**).[14,20−22] Besides the possibility of using the heavier Ge and Sn derivatives for further functionalization, *e.g.*, in established cross-coupling reactions, we were particularly interested in exploring the impact of these heavier atoms on the luminescence properties of the corresponding phospholes by systematic variation in the sequence Si, Ge, Sn. Moreover, their biological activity has led to increased interest in heterocyclic organogermanium compounds in the recent past.[23]

RESULTS AND DISCUSSION

Phosphole *via* Phosphanide Addition. The synthesis of the heavier tetryl phospholes was explored along the previously published route to silyl phospholes.[19] Therefore, in an initial step, the corresponding tetryl-substituted phosphanides were prepared *in situ*. To this end, phenylphosphane was lithiated with *n*-BuLi and reacted with Me_3ECl (E = Ge and Sn, Scheme 1). Subsequently, the reaction mixture was treated with another equivalent of *n*-BuLi and the diyne was added. The reaction was ended by adding a protic solvent (ethanol) to the reaction mixture. The ^{31}P NMR spectrum of crude germyl phosphole **1** shows a signal at δ 19.5 ppm (CD_2Cl_2), which is comparable to the corresponding β-silyl phosphole **IIIa** (δ 22.3 ppm).[17] Considering the successful preparation of germyl-substituted phosphole, we set out to explore the formation of the related stannyl-substituted compounds. Upon the addition of the corresponding trimethylstannyl phosphanide to the diyne (Scheme 1), a product was obtained with ^{31}P NMR resonance at δ 17.4 ppm and tin satellites with a $^{119/117}Sn$-coupling of 20.1 Hz. Unfortunately, compound **2** could not be isolated without the loss of the $SnMe_3$ group during the workup procedure. Nevertheless, the presence of **2** was proven

Received: January 12, 2023
Published: April 18, 2023

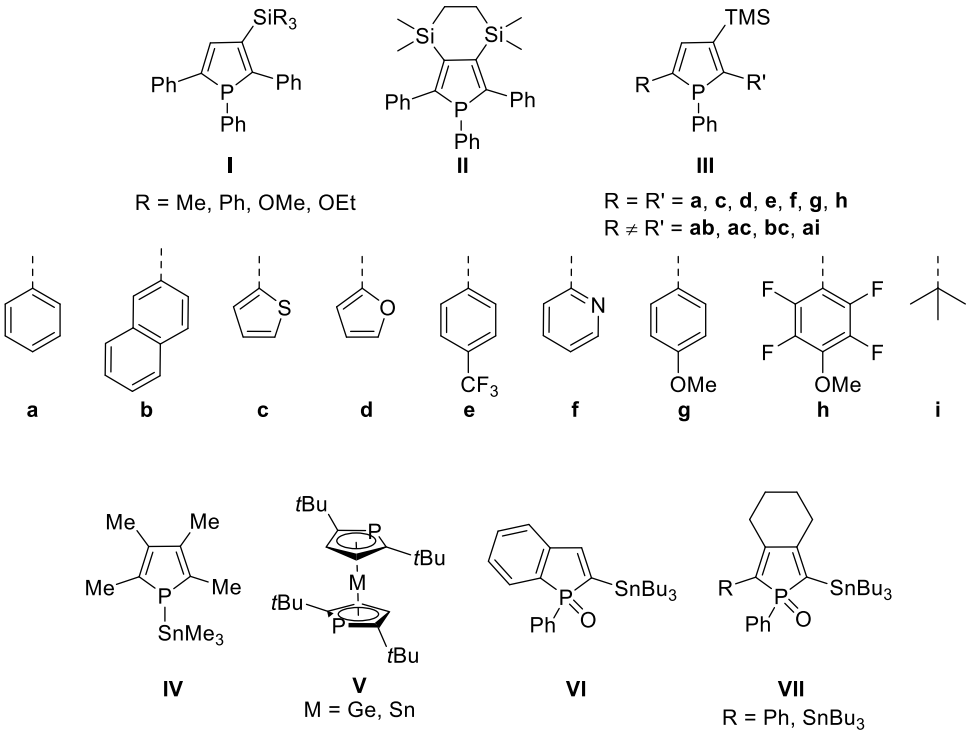

Figure 1. Top: general sketch of published β-substituted phospholes obtained *via* our previously reported method. Bottom: examples for reported Sn/Ge-substituted phosphole derivatives.

Scheme 1. Formation of β-Germyl and -Stannyl Phospholes 1 and 2 with Subsequent Oxidation of β-Germyl Phosphole 1 with O, S, and Se to O-1, S-1, and Se-1[a]

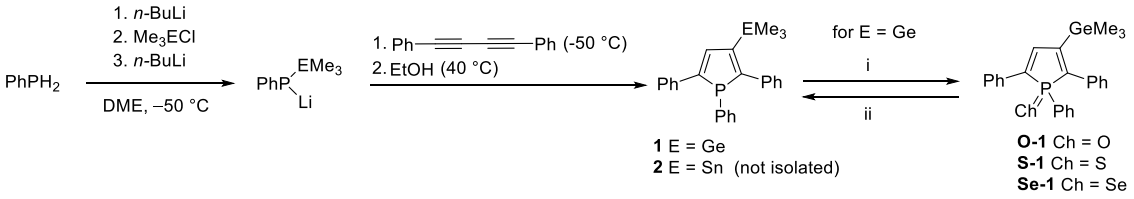

[a]i: 1 equiv H_2O_2, rt, 30 min (**O-1**); 1/8 S_8, rt, 16 h (**S-1**); 1 Se_{red}, rt, 16 h (**Se-1**), and reduction ii: 20 equiv LAH, 5 min in Et_2O, rt starting from phenylphosphane.

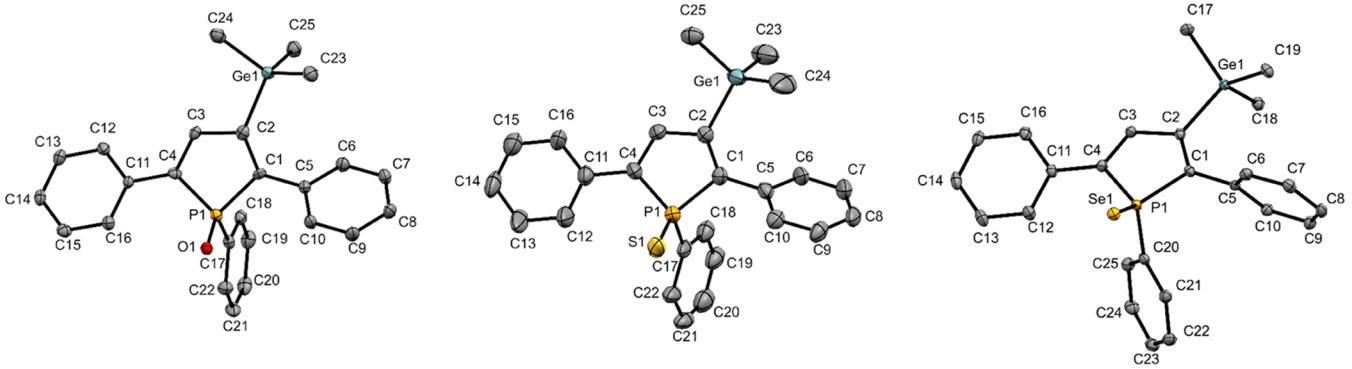

Figure 2. Molecular structures of β-germyl phosphole chalcogenides **O-1** (left), **S-1** (middle), and **Se-1** (right) in the solid state. Thermal ellipsoids were drawn at the 30% probability level. For clarity, hydrogen atoms have been omitted as well as disordered positions. Important bond lengths and angles of **O-1**: (C1)−(C2) 1.347(10) Å, (Ge1)−(C2) 1.976(7) Å, (C2)−(C3) 1.491(9) Å, (C3)−(C4) 1.350(9) Å, (C1)−(P1) 1.817(7) Å, (C4)−(P1) 1.804(7) Å, (C17)−(P1) 1.801(7) Å, (P1)−(O1) 1.482(4) Å; (C1)−(P1)−(C17) 108.9(3)°, (C4)−(P1)−(C17) 105.5(3)°, (C1)−(P1)−(C4) 93.4(3)°, (O1)−(P1)−(C17) 111.2(3) Å; **S-1**: (C1)−(C2) 1.346(12) Å, (Ge1)−(C2) 1.976(7) Å, (C2)−(C3) 1.469(12) Å, (C3)−(C4) 1.357(10) Å, (C1)−(P1) 1.824(7) Å, (C4)−(P1) 1.803(9) Å, (C17)−(P1) 1.846(11) Å, (P1)−(S1) 1.936(4) Å; (C1)−(P1)−(C17) 104.5(4)°, (C4)−(P1)−(C17) 107.6(5)°, (C1)−(P1)−(C4) 93.3(4)°, (S1)−(P1)−(C17) 115.4(4)°; **Se-1**: (C1)−(C2) 1.347(3)°, (Ge1)−(C2) 1.979(2) Å, (C2)−(C3) 1.480(3) Å, (C3)−(C4) 1.345(3) Å, (C1)−(P1) 1.821(2) Å, (C4)−(P1) 1.813(2) Å, (C20)−(P1) 1.816(3) Å, (P1)−(Se1) 2.108(1) Å; (C1)−(P1)−(C20) 106.7(1)°, (C4)−(P1)−(C20) 108.3(1)°, (C1)−(P1)−(C4) 92.9(1)°, (Se1)−(P1)−(C20) 114.0(1)°.

https://doi.org/10.1021/acs.organomet.3c00019
Organometallics 2023, 42, 793−802

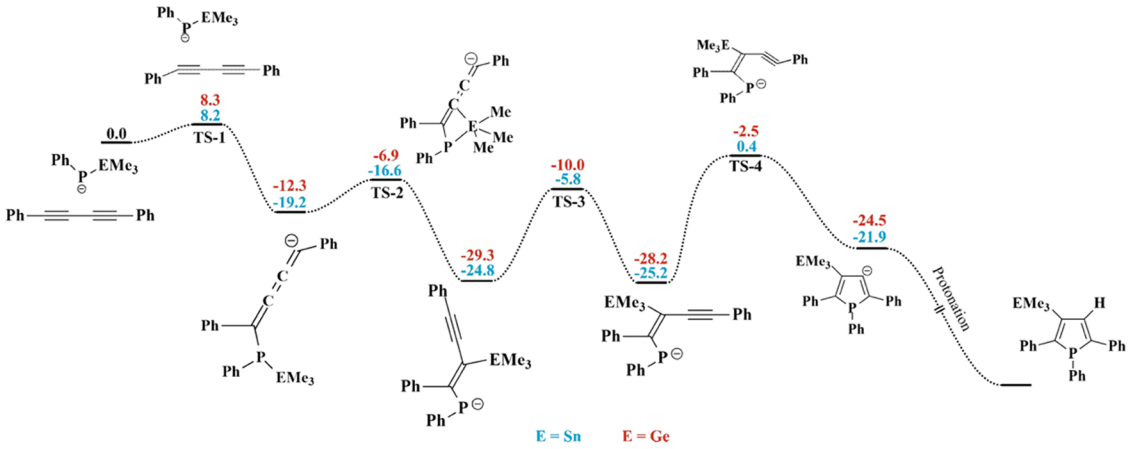

Figure 3. Postulated reaction mechanism calculated at ωB97X-D/6-311+G** (for Sn, the LANL2DZ basis set was used). The relative Gibbs free energy values are in kcal/mol unit.

by mass spectrometry (for ESI-MS of **2**, *cf.* Supporting Information).

Attempted purification of crude phospholes **1** and **2** *via* column chromatography entailed some difficulties. For the germanium derivative, similar polarities of the diyne reactant and the desired product precluded proper separation. Therefore, germyl phosphole **1** was oxidized *in situ* with H_2O_2, sulfur, or red selenium, and the resulting chalcogenophospholes **O-1**-**Se-1** (Scheme 1) could be purified and isolated *via* chromatography. By contrast, stannyl phosphole **2** turned out to be sensitive even toward silica gel deactivated with Et_3N, whereas with alumina as the stationary phase, no separation could be achieved. Likewise, the higher reactivity of the tin−carbon bond did not allow the controlled formation of the respective chalcogenide derivatives for improved polarity differences.

The obtained germanium-based phosphole chalcogenides (**O-1**-**Se-1**) show singlet resonances in the ^{31}P NMR spectra at δ 43.6, 55.0, and 43.8 ppm, respectively, which are shifted by approximately 2 ppm to a higher field compared with the respective β-silyl phosphole chalcogenides. The ^{77}Se NMR spectrum of **Se-1** shows a doublet at δ −408 (^1J = 743 Hz), which is identical to the known β-silyl phosphole derivative suggesting comparable basicity of the lone pair of the underlying phosphole.[17] Suitable crystals for X-ray measurement could be obtained in case of all oxidized phosphole derivatives, which verified the chemical composition of these compounds and allowed the investigation of the molecular structures of these systems in the solid state (Figure 2). To the best of our knowledge, these are the first germanium derivatives of phospholes being structurally characterized in the solid state. The germyl groups induce a twisting of the neighboring ring adjacent to the phosphole's α-position, similar to the one described for β-silyl phospholes **III** (Figure 1). The twisting increases with a higher atomic number of the chalcogen atom from 38.6(2)° in oxygen-based **O-1** over 47.2(3)° in sulfur-based **S-1** to 82.5(1)−83.3(1)° in selenium-based **Se-1**. The phenyl substituents not directly neighboring the germyl group show a smaller twisting of 17.7(2)° (**O-1**), 5.2(4)° (**S-1**), and 1.4(1)−15.2(1)° (**Se-1**). Compared to the β-silyl phosphole oxide, the angles found here are about 2° smaller.[17] The bond distance of the Ge1−C2 bond is similar in all structures (1.976(7)−1.979(2) Å).

Reduction of the corresponding phosphole chalcogenides **O-1** through **Se-1** has been investigated with $(SiCl_3)_2$ in a dichloromethane solution following known protocols.[24−26] Interestingly, the reduction was either nonselective or a heterolytic cleavage of the germanium−carbon bond was observed. Therefore, the halide-free reducing agent $LiAlH_4$ (LAH) was used instead,[27] for which selective formation of compound **1** was observed within five minutes, as followed by ^{31}P NMR spectroscopy.

Our experimental findings indicate that germyl and stannyl phosphanides can add to diynes with subsequent phosphole formation in a similar fashion as silylphosphanides. Therefore, we aimed to compare the mechanism of their formation with the silyl-substituted derivative, which has been investigated in detail in our previous work.[19] Our density functional theory (DFT) study showed that the reaction pathway is very similar to the parent silyl-substituted derivative (Figure 3). The corresponding phosphanide anion attacks one of the triple bonds of the diyne; this step has a low barrier in both cases. The following step is the migration of the germyl/stannyl group, which has a very low barrier in both cases ($\Delta G^{\#}$ = 5.4 kcal/mol for E = Ge and $\Delta G^{\#}$ = 2.6 kcal/mol for E = Sn). Apart from the fact that the C−E bond is more stable than the P−E bond (E = Ge, Sn), the thermodynamic sink of the process is the formation of a delocalized system (1-phosphaallylic anion), where the negative charge is distributed (Figure S45). Indeed, the high degree of delocalization lends high stability to these intermediates. On the other hand, this intermediate has *Z*-configuration; therefore, it is not ready for ring closure. The corresponding *E*-isomer, which is ready to undergo ring-closing, is accessible *via* a medium-high barrier (19.3 and 19.0 kcal/mol), while the ring closure has a somewhat higher barrier (25.7 and 25.6 kcal/mol), compared to the other step of the mechanism. After protonation, the corresponding phosphole forms, which is more stable by 37.0 kcal/mol (E = Ge) and 36.6 kcal/mol (E = Sn) than the corresponding protonated 1-phosphaallylic anion derivatives (Table S4 in the Supporting Information).

Phosphole *via* Zirconacycle. Since the phosphanide addition was only partly successful in the preparation of stannyl-substituted phospholes, we considered an alternative strategy to get to these compounds using the well-established method by Fagan and Nugent.[28] Here, bissilyl phospholes have been reported where regioselectivity of the silyl groups has

https://doi.org/10.1021/acs.organomet.3c00019
Organometallics 2023, 42, 793−802

Scheme 2. Preparation of 2,4-Bisstannyl Phosphole Derivatives Form Ethynylstannes 3a-c with R = Methyl (Me, a), *n*-Butyl (*n*-Bu, b), and Phenyl (Ph, c)[a]

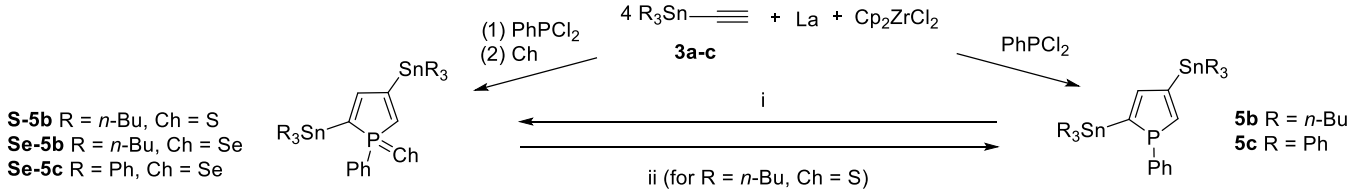

[a]Reaction conditions: **S-5b** (Ch═S) and **Se-5c**, (Ch═Se) i: 1/8 S_8, rt, 16 h (**S-5b**) 1 Se_{red}, rt, 16 h (**Se-5c**), and reduction ii: 1.5 equiv $(SiCl_3)_2$, toluene-d_8,16 h, rt (**5b**).

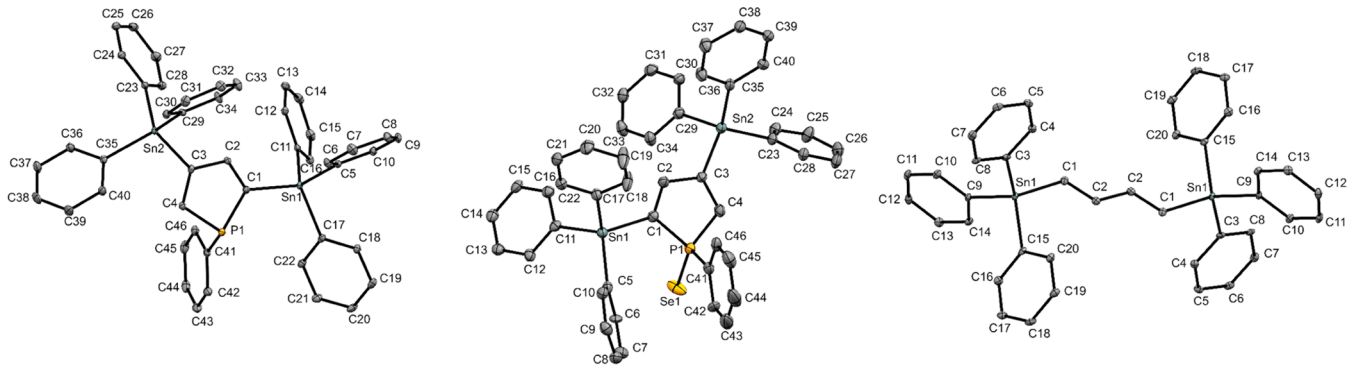

Figure 4. Molecular structures of **5c** (left), **Se-5c** (middle), and **4c** (right) in the solid state. Thermal ellipsoids were drawn at the 30% probability level. For clarity, hydrogen atoms have been omitted as well as disordered positions. Important bond lengths and angles of **5c**: (C1)−(C2) 1.350(4) Å, (C2)−(C3) 1.458(3) Å, (C3)−(C4) 1.356(4) Å, (C1)−(P1) 1.790(3) Å, (C4)−(P1) 1.793(3) Å, (P1)−(C41) 1.823(3) Å, (C1)−(Sn1) 2.132(2) Å, (C2)−(Sn2) 2.128(3) Å, (Sn1)−(C5) 2.137(3) Å, (Sn1)−(C11) 2.139(3) Å, (Sn1)−(C17) 2.138(3) Å, (Sn2)−(C23) 2.135(3) Å, (Sn2)−(C29) 2.134(3) Å, (Sn2)−(C35) 2.124(2)°; (C1)−(P1)−(C41) 106.5(1)°, (C4)−(P1)−(C41) 105.9(1)°, (C1)−(P1)−(C4) 91.2(1) Å, (C1)−(Sn1)−(C5) 106.9(1) Å, (C5)−(Sn1)−(C17) 106.6(1) Å, (C5)−(Sn1)−(C11) 110.0(1)°, (C29)−(Sn2)−(C35) 112.9(1)°, (C3)−(Sn2)−(C23) 107.1(1)°, (C23)−(Sn2)−(C35) 110.1(1)°; **Se-5c**: (C1)−(C2) 1.319(2) Å, (C2)−(C3) 1.515(1) Å, (C3)−(C4) 1.351(2) Å, (C1)−(P1) 1.811(1) Å, (C4)−(P1) 1.798(1) Å, (P1)−(C41) 1.802(1) Å, (C1)−(Sn1) 2.154(9) Å, (C2)−(Sn2) 2.104(10) Å, (Sn1)−(C5) 2.121(12) Å, (Sn1)−(C11) 2.139(12) Å, (Sn1)−(C17) 2.117(14) Å, (Sn2)−(C23) 2.133(10) Å, (Sn2)−(C29) 2.117(12) Å, (Sn2)−(C35) 2.118(13) Å, (P1)−(Se1) 2.098(6) Å; (C1)−(P1)−(C41) 105.8(5)°, (C4)−(P1)−(C41) 109.2(6)°, (C1)−(P1)−(C4) 92.6(6)°, (C1)−(Sn1)−(C5) 110.3(4)°, (C5)−(Sn1)−(C17) 107.9(5)°, (C5)−(Sn1)−(C11) 113.8(5)°, (C29)−(Sn2)−(C35) 111.4(5)°, (C3)−(Sn2)−(C23) 109.9(4)°, (C23)−(Sn2)−(C35) 110.1(4)°, (C41)−(P1)−(Se1) 114.7(4)°; **4c**: (Sn1)−(C1) 2.101(6) Å, (Sn1)−(C3) 2.162(5) Å, (Sn1)−(C9) 2.134(6) Å, (Sn1)−(C15) 2.128(7)°, (C2)−(C2) 1.464(11) Å; (C1)−(Sn1)−(C15) 108.3(3)°, (C3)−(Sn1)−(C15) 107.9(2)°, (C3)−(Sn1)−(C9) 111.8(2)°, (C9)−(Sn1)−(C15) 108.4(3).

Table 1. Selected Bond Lengths and Angles for 5c and Se-5c

	5c	Se-5c
Σ(∢P) [°]	303.6(2)	
C-Sn-C bond angle [°]	106.6 - 112.9	107.9 - 113.8
Sn-C bond length [Å]	2.124(2) - 2.139(3)	2.104(10) - 2.154(9)
P-Se- bond length [Å]	-	2.098(6)

been achieved.[29,30] Therefore, we adapted this approach using stannyl-substituted terminal alkynes with differently substituted stannyl groups (Scheme 2; R = methyl (Me, **a**), *n*-butyl (*n*-Bu, **b**), and phenyl (Ph, **c**)). We found a significant impact of the substituents of the stannyl group on the reaction outcome. With Me-substituted ethynylstannane being insoluble, a possibly polymeric material was obtained instead of the envisaged phosphole **5a**. By contrast, with *n*-Bu- or Ph-substituted ethynylstannanes, the respective bisstannyl phospholes **5b,c** have been obtained regioselectively. The ^{31}P NMR spectra in the CD_2Cl_2 solution show singlet resonances at δ 37.0 ppm (**5b**) and δ 35.3 ppm (**5c**). While *n*-Bu-substituted **5b** is very sensitive toward oxidation, phenyl-substituted **5c** is air-stable and was obtained in good yield (74%). During the synthesis of **5c**, the formation of the byproduct $(Ph_3SnCH{=}CH)_2$ (**4c**) has been observed, which could be separated from **5c** *via* fractional crystallization. The rather limited efficiency of this procedure was found to be improved for its selenium derivative **Se-5c** owing to the larger difference in polarity. Most efficiently, **5c** and **Se-5c** have been purified *via* column chromatography. By contrast, purification of the tributylstannyl-substituted phosphole **5b** *via* chromatography turned out to be difficult but could be achieved for the respective phosphole chalcogenides obtainable by direct oxidation of the crude product mixture with elemental sulfur or red selenium. After successful purification, sulfide **S-5b** was isolated as a yellow oil,

https://doi.org/10.1021/acs.organomet.3c00019
Organometallics 2023, 42, 793−802

Table 2. Summarized NMR Data of 5b, S-5b, Se-5b, 5c, and Se-5c Recorded in CD_2Cl_2

	5b	S-5b	Se-5b	5c	Se-5c
^{31}P NMR [ppm]	37.0	63.9	50.6	35.3	52.5
coupling [Hz]	$^2J_{P-^{119/117}Sn}$ = 54	$^2J_{P-^{117}Sn}$ = 128	$^2J_{P-^{117}Sn}$ = 128	$^2J_{P-^{119/117}Sn}$ = 70	$^2J_{P-^{117}Sn}$ = 176
	$^3J_{P-^{117}Sn}$ = 173	$^2J_{P-^{119}Sn}$ = 131	$^2J_{P-^{119}Sn}$ = 132	$^3J_{P-^{117}Sn}$ = 209	$^2J_{P-^{119}Sn}$ = 184
	$^3J_{P-^{119}Sn}$ = 177	$^3J_{P-^{117}Sn}$ = 172	$^3J_{P-^{117}Sn}$ = 184	$^3J_{P-^{119}Sn}$ = 219	$^3J_{P-^{117}Sn}$ = 208
		$^3J_{P-^{119}Sn}$ = 176	$^3J_{P-^{119}Sn}$ = 208		$^3J_{P-^{119}Sn}$ = 218
^{119}Sn NMR [ppm]		−38, −46	−38, −47	−131, −145	−138, −148
^{77}Se NMR [ppm]			−478		−479
coupling [Hz]			$^1J_{Se-^{31}P}$ = 714		$^1J_{Se-^{31}P}$ = 725

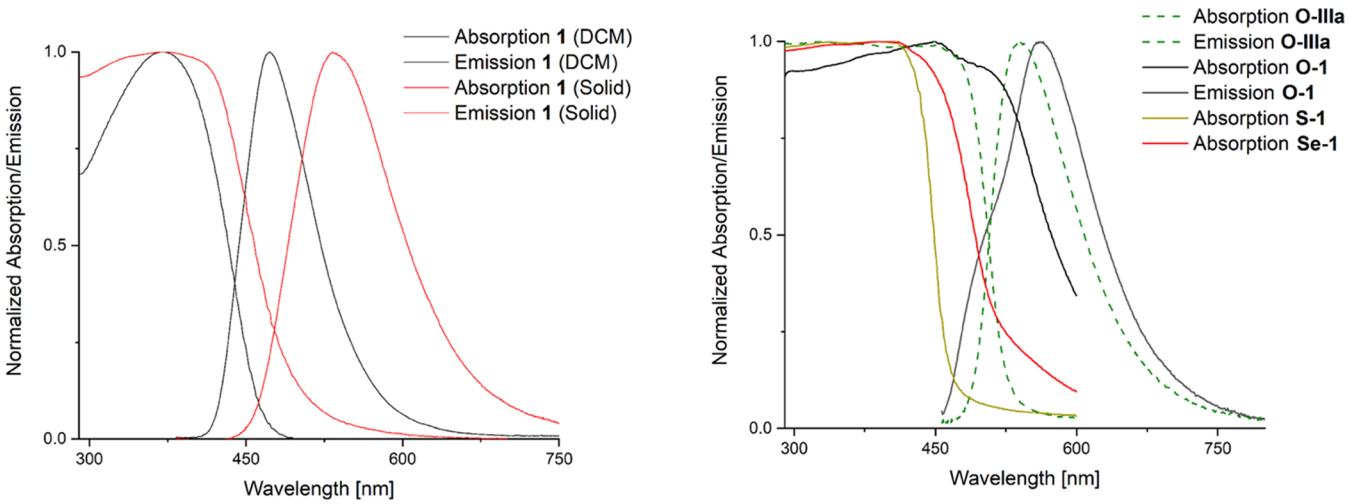

Figure 5. Normalized absorption and emission spectra of β-germyl phosphole **1** in the solid state and solution (DCM) and of β-germyl phosphole chalcogenides **O-1**−**Se-1** and their analogous β-TMS derivative **O-IIIa** in the solid state.

while selenium derivative **Se-5b** showed an orange color. From these chalcogenides, the corresponding phosphole **5b** has been regenerated *via* reduction with excess $(SiCl_3)_2$ at room temperature in a toluene solution. Nevertheless, **5b** was still contaminated with the starting phosphole chalcogenide. Regeneration of **5c** from **Se-5c** is feasible as well, however, of limited synthetic use, as **5c** can be purified directly *via* chromatography. For compounds **5c**, **Se-5c**, and **4c**, the molecular structures in the solid state have been determined *via* SCXRD (Figure 4). The tin atoms in bisstannyl phosphole **5c**, selenide **Se-5c**, and diene **4c** adopt a distorted tetrahedral environment (Table 1). The bond lengths of the Sn−C bonds lie below the van der Waals radii of the atoms involved.[31] In **5c**, the phosphorus atom adopts a distorted trigonal pyramidal geometry, whereas the oxidized derivative **Se-5c** inhibits a distorted tetrahedral geometry. In **4c**, the Ph_3Sn substituents adopt a gauche conformation to each other.

The NMR data of compounds **5b,c** are summarized in Table 2. **5c** shows a signal with two pairs of tin satellites at δ 35.3 ppm $^2J_{P-^{119/117}Sn}$ = 70 Hz, $^3J_{P-^{117}Sn}$ = 209 Hz, and $^3J_{P-^{119}Sn}$ = 219 Hz in the ^{31}P NMR spectrum. ^{119}Sn{^{1}H} NMR shows two doublets at δ −131 and −145 ppm with the corresponding coupling constants. Close by but easy to distinguish, byproduct **4c** features a single resonance at δ −143 ppm in the ^{119}Sn NMR spectra. For chalcogenide **Se-5c**, the signal is more deshielded and shifted to δ 52.5 ppm with larger coupling constants ranging between 176 and 218 Hz. The *n*-butyl derivatives **5b**, **S-5b**, and **Se-5b** show comparable chemical shifts and coupling constants to phenyl-substituted **5c** and **Se-5c**, which are also consistent with the literature.[22] By contrast, a comparison of the ^{77}Se coupling constants for **Se-5b** and **Se-5c** show lower values than for most other phosphole selenides found in the literature. In germyl-substituted **Se-1**, the value of the coupling constant is 743 Hz which is larger than in bisstannyl-substituted **Se-5b** (714 Hz) and **Se-5c** (725 Hz), as well as in already reported 1-phenyl-2,4-bis(trimethylsilyl)-phosphole selenide (716 Hz)[29] albeit in a different solvent ($CDCl_3$). This comparison suggests a high basicity of the lone pair at the phosphorus atom in the underlying germyl phosphole **1**, which could be interesting regarding its coordination properties in future investigations.

Photophysical Properties. Given the luminescent properties of many phospholes and their derivatives, we wanted to explore the photophysical properties of the new germyl- and stannyl-substituted phosphole derivatives, namely, **1**, **O-1**, **S-1**, **Se-1**, **5b**, and **5c** (Figure 5). Compound **1** shows comparable absorption maxima in solution (DCM) and the solid state (370 and 373 nm, respectively). The quantum yields are similar in both solution and the solid state as well (13 and 14%, respectively). Only the emission maxima differ significantly with red-shifted emission in the solid (472 *vs* 532 nm, respectively). Compared to the previously published β-TMS phosphole **IIIa**, its germanium analogue **1** shows very similar photophysical properties in solution, which is quite remarkable since formally, a 3rd-row element (Si) is replaced by a 4th-row element (Ge) for which fluorescence quenching owing to the heavy atom would be anticipated. In the solid state, the situation is more complex; while the absorption maximum of **IIIa** at 375 nm is similar to **1**, the Stokes shift of the silyl phosphole is much smaller compared with the germyl

https://doi.org/10.1021/acs.organomet.3c00019
Organometallics 2023, 42, 793−802

phosphole (6006 *vs* 8013 cm^{-1}, respectively), and the quantum yield, on the other hand, is much higher (82%).[18] Also referring to the solid state, the oxidized germyl phosphole **O-1** exhibits an intense absorption band at 450 nm, which is blue-shifted with respect to the nonoxidized phosphole **1**, yet almost identical to that of the literature-known silicon analogue **O-IIIa**. For the heavier chalcogen derivatives, **S-1** and **Se-1**, the absorption bands are shifted further to shorter wavelengths (430 and 432 nm, respectively). In the case of **5b** and **5c**, no luminescence was found in the solid state or solution. TD-DFT calculations (Table S5) have demonstrated that the observed absorption maxima are mainly due to the highest occupied molecular orbital (HOMO)−lowest unoccupied molecular orbital (LUMO) transitions in the case of **1** and **O-1**, while in the case of **S-1** and **Se-1**, the transition from HOMO-1 and HOMO-2 has a significant contribution as well (Table S5 in the Supporting Information). Since both the HOMO and LUMO (Figure 6) are localized mainly at the phosphole unit

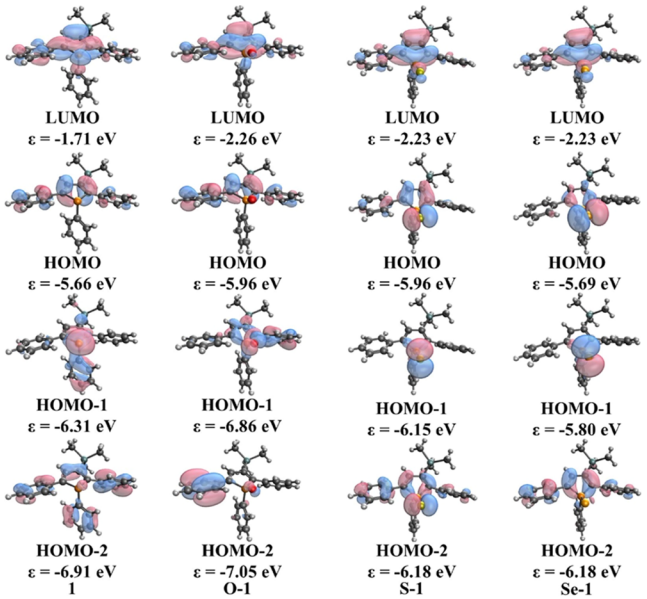

Figure 6. Selected Kohn−Sham orbitals of **1**, **O-1**, **S-1**, and **Se-1** at the B3LYP/6-31G*//ωB97X-D/6-311+G** level of theory.

in the case of **1** and **O-1**, the corresponding electron excitations could be considered as local $\pi \rightarrow \pi^*$ transitions. On the other hand, in the case of **S-1** and **Se-1**, transitions from the HOMO-1 and HOMO-2 may lend some charge transfer (CT) character (from the chalcogen toward the phosphole unit) of these excitations since the lone pairs of the chalcogen atoms have major contributions to the above-mentioned occupied orbitals. In the case of **5b**, the π-system of the ring has a main contribution to the HOMO, while HOMO-1 is basically the lone pair of the phosphorus atom (Figure S46 in the Supporting Information). The energy order of these two orbitals changes in the case of **5c**.

Investigating the luminescence of the above-discussed compounds, it can be established that **O-1** shows no luminescence in solution, whereas, in the solid state, the compound is luminescent with a 22% quantum yield, which indicates aggregation-induced emission. Similar behavior has been observed for silyl-substituted phosphole oxides, with hindered rotation of the nonplanar fluorophore in the solid as a potential explanation,[32] as is established for various molecular scaffolds.[33−38] The quantum yield of the germanium compound is 7% higher than that of its literature-known silicon analogue **O-IIIa**. Both emission spectra were recorded with an excitation wavelength of 450 nm. The corresponding emission maxima were detected at 560 nm for **O-1** and blue-shifted by 20 nm for the reference substance (Figure 5). The absorption, on the other hand, is much broader for the germanium derivative. The point where the absorption drops to 50% is red-shifted by 67−573 nm compared to 506 nm for the TMS derivative.

In contrast to **1** and **O-1**, no fluorescence was found for **S-1** and **Se-1**, which was also mentioned for the chalcogen derivatives o the 1,2,5-triphenyl-1*H*-phosphole. According to the literature, the suppression of fluorescence could be induced by a higher spin−orbit coupling for the heavier chalcogenides.[39] Analogous to these findings, also the tin-based phospholes **5b** and **5c** show no emission, which in these cases could be justified by the increased number of degrees of freedom in these molecules.

CONCLUSIONS

In conclusion, we have prepared and isolated the first germyl-substituted phosphole **1** and its chalcogen (O, S, Se) derivatives **O-1** to **Se-1**. The increased reactivity of the Ge−C bond, as compared to Si−C, in the phosphole did not allow direct purification *via* chromatography. The corresponding chalcogen derivatives were more robust and thus purification and subsequent reduction back to **1** turned out to be a successful synthetic pathway. In the DCM solution, the photophysical properties of **1** are almost interchangeable with that of its silyl-substituted analogue, whereas, in the solid state, the germyl phosphole shows lower quantum yields and a larger Stokes shift. Our attempts to prepare an analogous stannyl-substituted phosphole were only partly successful. Formation of **2** has been confirmed by ^{31}P NMR spectroscopy and mass spectrometry; however, isolation of the pure compound failed in our hands. The higher reactivity of the tin−carbon bond did not allow the formation of the corresponding chalcogenides, as in the germanium case. By contrast, the Fagan−Nugent approach gave access to bisstannyl phospholes **5b,c** in a regioselective manner. These bisstannylated phospholes show no detectable luminescence but may be useful precursors for embedding phospholes into more extended molecules *via* cross-coupling reactions in future studies.

EXPERIMENTAL SECTION

General. All reactions were carried out by means of standard Schlenk or glovebox techniques under an inert gas atmosphere (argon) when necessary. Solvents were dried over a Na/K alloy before use and were freshly distilled under inert gas. Phenylphosphane ($PhPH_2$) has been prepared following the literature procedure.[40] 1,4-diphenyllbutadiyne was synthesized according to the literature.[41] Deuterated solvents for NMR spectroscopy were dried and stored over molecular sieves. All chemicals were purchased from Sigma-Aldrich, ABCR, or TCI and used without further purification. For purification *via* column chromatography, a puriFlash XS 520 plus (Interchim) was used. The used cartridges were filled with spheric silica gel (particle size: 15 or 25 μm). ^{1}H, ^{13}C, ^{31}P, ^{29}Si, ^{77}Se, and ^{119}Sn NMR data were recorded on a Varian VNMRS-500 or MR-400 MHz spectrometer at 25 °C. Chemical shifts were referenced to residual protic impurities in the solvent (^{1}H) or the deuterated solvent (^{13}C) and reported relative to external $SiMe_4$ (^{1}H, ^{13}C, ^{29}Si), H_3PO_4 (^{31}P), Me_2Se (^{77}Se) and $SnMe_4$ (^{119}Sn). APCI mass determinations

https://doi.org/10.1021/acs.organomet.3c00019
Organometallics 2023, 42, 793−802

were performed on a Finnigan LCQ Deca (ThermoQuest). Mass calibration was carried out immediately before sample measurement on sodium formate clusters or by the ESI-Tune Mix standard (Agilent). Elemental analyses were performed with a HEKAtech Euro EA CHNS elemental analyzer. Samples were prepared in an Sn cup and analyzed with added V_2O_5. Absorption spectra were recorded using a Shimadzu UV-1900 spectrometer in solution. Emission spectra, as well as luminescence quantum yields (absolute method), were measured with the Hamamatsu C11347 system in solution. For the refinement of the data, OriginPro was used. Crystallographic measurements were carried out on a STOE IPDS2 diffractometer with an STOE image plate detector and a Mo Kα (λ = 0.71073 Å) monochromator or a STOE StadiVari diffractometer with a Pilatus 200K image plate detector and Cu Kα (λ = 1.54186 Å) radiation. Direct methods were used to solve the measurements and refined by "least-square" cycles (SHELXL-2017).[42] All non-hydrogen atoms were anisotropically refined without restriction. The evaluation of the data sets, as well as the graphical preparation of the structures, was carried out using Olex2[43] and Mercury.[44] Details of the structure determinations and refinement are summarized in Tables S1 and S2. The CCDC depositions 2223036−2223041 contain the supplementary crystallographic data for this paper, which can be obtained free of charge *via* emailing data_request@ccdc.cam.ac.uk, or by contacting The Cambridge Crystallographic Data Centre at 12 Union Road, Cambridge CB2 1EZ, U.K.; fax: +44 1223 336033.

Synthetic Protocols and Characterization. *Synthesis of 1,2,5-Triphenyl-3-(trimethylgermyl)-1H-phosphole (**1**).* A Schlenk tube filled with phosphole **Se-1** (50.8 mg, 0.1 mmol, 1 equiv) and LAH (75.9 mg, 20 mmol, 20 equiv) was charged with Et_2O (5 mL) and stirred for 5 min at rt. Afterward, additional LAH was filtered and the solvent was removed under reduced pressure. The obtained residue was extracted with pentane, and after evaporation of the solvent, compound **1** was obtained as a greenish wax. Yield: 82% (35.2 mg). **^{1}H NMR** (499.75 MHz, CD_2Cl_2) δ = 7.56−7.55 (m, 2H, 2× CH_{Ar}), 7.39 (d, $^3J(^1H\text{-}^{31}P)$ = 10.3 Hz, 1H, $(CH_3)_3GeCCH$), 7.32−7.15 (m, 13 H, 13× CH_{Ar}), 0.27 (s, 9H, 3× Ge(CH_3)). **^{13}C{^{1}H} NMR** (100.56 MHz, CD_2Cl_2) δ = 161.5 (d, $J(^{13}C\text{-}^{31}P)$ = 5.6 Hz, C_q), 151.0 (d, $J(^{13}C\text{-}^{31}P)$ = 3.0 Hz, C_q), 149.5 (d, $J(^{13}C\text{-}^{31}P)$ = 5.1 Hz, C_q), 139.3 (d, $J(^{13}C\text{-}^{31}P)$ = 20.1 Hz, C_q), 137.9 (d, $J(^{13}C\text{-}^{31}P)$ = 13.0 Hz, CH), 137.2 (d, $J(^{13}C\text{-}^{31}P)$ = 15.9 Hz, C_q), 134.2 (d, $J(^{13}C\text{-}^{31}P)$ = 18.9 Hz, CH), 131.4 (d, $J(^{13}C\text{-}^{31}P)$ = 10.8 Hz, C_q), 130.0 (s, CH), 129.5 (d, $J(^{13}C\text{-}^{31}P)$ = 8.2 Hz, CH), 129.4 (s, CH), 129.2 (s, CH), 129.2 (s, CH), 129.1, (s, CH), 128.5 (s, CH), 127.6 (s, CH), 127.0 (d, $J(^{13}C\text{-}^{31}P)$ = 9.4 Hz, CH), 0.4 (s, Ge(CH_3)$_3$). **^{31}P NMR** (202.30 MHz, CD_2Cl_2) δ = 19.4 (s). **MS** (APCI-LR) *m*/*z*: found: 431.00. [**1** + H]$^+$, calcd for $C_{25}H_{26}GeP$: 431.10. Elemental analysis (%): calcd for $C_{25}H_{25}GeP$: C 69.98, H 5.87 found: C 69.98, H 6.11.

*Synthesis of 1,2,5-Triphenyl-3-(trimethylgermyl)-1H-phosphole-1-oxide (**O-1**).* A Schlenk tube was charged with DME (20 mL) and cooled to −70 °C. Then, phenylphosphane (0.11 g, 1 mmol, 1.0 equiv) was added. After that, *n*BuLi (2.5 M, 0.42 mL, 1,05 mmol, 1.05 equiv) was used for lithiation. The orange solution was stirred for 30 min and quenched with chlorotrimethylgermane (0.12 mL, 1 mmol, 1 equiv). The colorless solution was lithiated with *n*BuLi (2.5 M, 0.42 mL, 1.05 mmol, 1.05 equiv) again. After 45 min, 1,4-diphenylbuta-1,3-diyne (0.202 g, 1 mmol, 1 equiv) dissolved in DME (10 mL) was added dropwise to the orange solution. The color changed to deep blue, and after 80 min, the reaction mixture was warmed up to 40 °C and stirred for 10 min. The reaction was terminated by adding ethanol. Afterward, the solvent was removed, and the crude product was suspended in 20 mL of DCM. After that, an excess of H_2O_2 was added and the suspension was stirred for 16 h at rt. The crude product was purified by silica gel column chromatography with dichloromethane. The product was obtained as an orange solid. Yield: 63% (0.278 g). **^{1}H NMR** (499.75 MHz, CD_2Cl_2) δ = 7.75−7.71 (m, 2 H, 2× CH_{Ar}), 7.64−7.62 (m, 2H, 2× CH_{Ar}), 7.49−7.46 (m, 1H, 1× CH_{Ar}), 7.42−7.38 (m, 2H, 2× CH_{Ar}), 7.40 (d, $^3J(^1H\text{-}^{31}P)$ = 36.8 Hz, 1H, $(CH_3)_3GeCCH$), 7.33−7.23 (m, 8H, 8× CH_{Ar}), 0.29 (s, 9H, 3× Ge(CH_3)). **^{13}C{^{1}H} NMR** (100.56 MHz, CD_2Cl_2) δ = 153.4 (d, $J(^{13}C\text{-}^{31}P)$ = 15.4 Hz, C_q), 147.8 (d, $J(^{13}C\text{-}^{31}P)$ = 85.5 Hz, C_q), 137.9 (d, $J(^{13}C\text{-}^{31}P)$ = 34.6 Hz, CH), 137.2 (d, $J(^{13}C\text{-}^{31}P)$ = 96.8 Hz, C_q), 135.4 (d, $J(^{13}C\text{-}^{31}P)$ = 13.9 Hz, CH), 133.0 (d, $J(^{13}C\text{-}^{31}P)$ = 12.6 Hz, C_q), 132.5 (d, $J(^{13}C\text{-}^{31}P)$ = 2.9 Hz, CH), 130.9 (d, $J(^{13}C\text{-}^{31}P)$ = 10.4 Hz, CH), 129.5 (d, $J(^{13}C\text{-}^{31}P)$ = 87.5 Hz, C_q), 129.5 (d, $J(^{13}C\text{-}^{31}P)$ = 11.8 Hz, CH), 129.4 (s, CH), 129.2 (s, CH), 128.9 (d, $J(^{13}C\text{-}^{31}P)$ = 4.2 Hz, CH), 128.8 (s, CH), 128.7 (s, CH), 126.8 (d, $J(^{13}C\text{-}^{31}P)$ = 5.9 Hz, CH), −0.6 (s, Ge(CH_3)$_3$). **^{31}P NMR** (202.30 MHz, CD_2Cl_2) δ = 43.5 (s). **MS** (APCI-LR) *m*/*z*: found: 447.07. [**O-1** + H]$^+$, calcd for $C_{25}H_{26}GeOP$: 447.09. Elemental analysis (%): calcd for $C_{25}H_{25}GeOP$: C 67.47, H 5.66 found: C 67.66, H 5.80.

*Synthesis of 1,2,5-Triphenyl-3-(trimethylgermyl)-1H-phosphole-1-sulfide (**S-1**).* A Schlenk tube was charged with DME (20 mL) and cooled to −70 °C. Then, phenylphosphane (0.11 g, 1 mmol, 1.0 equiv) was added. After that, *n*BuLi (2.5 M, 0.42 mL, 1,05 mmol, 1.05 equiv) was used for lithiation. The orange solution was stirred for 30 min and quenched with chlorotrimethylgermane (0.12 mL, 1 mmol, 1 equiv). The colorless solution was lithiated with *n*BuLi (2.5 M, 0.42 mL, 1.05 mmol, 1.05 equiv) again. After 45 min, 1,4-diphenylbuta-1,3-diyne (0.202 g, 1 mmol, 1 equiv), dissolved in DME (10 mL), was added dropwise to the orange solution. The color changed to deep blue, and after 80 min, the reaction mixture was warmed up to 40 °C and stirred for 10 min. The reaction was terminated by adding ethanol. Afterward, an excess of elemental sulfur (96 mg, 3 mmol, 3 equiv) was added and the suspension was stirred for 16 h at rt. The crude product was purified by silica gel column chromatography with *n*-pentane/dichloromethane 1:1. The product was obtained as a yellow solid. Yield: 63% (0.289 g). **^{1}H NMR** (499.75 MHz, CD_2Cl_2) δ = 7.89−7.85 (m, 2H, 2× CH_{Ar}), 7.67−7.65 (m, 2H, 2× CH_{Ar}), 7.52−7.43 (m, 3H, 3× CH_{Ar}), 7.50 (d, $^3J(^1H\text{-}^{31}P)$ = 36.0 Hz, 1 H, $(CH_3)_3GeCCH$), 7.34−7.27 (m, 6H, 6× CH_{Ar}), 7.21−7.19 (m, 2H, 2× CH_{Ar}), 0.30 (s, 9H, 3× Ge(CH_3)). **^{13}C{^{1}H} NMR** (100.56 MHz, CD_2Cl_2) δ = 153.2 (d, $J(^{13}C\text{-}^{31}P)$ = 11.9 Hz, C_q), 151.3 (d, $J(^{13}C\text{-}^{31}P)$ = 67.2 Hz, C_q), 140.5 (d, $J(^{13}C\text{-}^{31}P)$ = 81.7 Hz, C_q), 138.0 (d, $J(^{13}C\text{-}^{31}P)$ = 31.4 Hz, CH), 134.8 (d, $J(^{13}C\text{-}^{31}P)$ = 15.4 Hz, C_q), 132.7 (d, $J(^{13}C\text{-}^{31}P)$ = 13.4 Hz, C_q), 132.6 (d, $J(^{13}C\text{-}^{31}P)$ = 3.0 Hz, CH), 130.9 (d, $J(^{13}C\text{-}^{31}P)$ = 11.7 Hz, CH), 129.7 (d, $J(^{13}C\text{-}^{31}P)$ = 4.0 Hz, CH), 129.5 (d, $J(^{13}C\text{-}^{31}P)$ = 12.3 Hz, CH), 129.3 (s, CH), 129.2 (s, CH), 128.9 (d, $J(^{13}C\text{-}^{31}P)$ = 2.0 Hz, CH), 128.5 (d, $J(^{13}C\text{-}^{31}P)$ = 1.3 Hz, CH), 127.5 (d, $J(^{13}C\text{-}^{31}P)$ = 69.9 Hz, C_q), 127.2 (d, $J(^{13}C\text{-}^{31}P)$ = 6.1 Hz, CH), −0.5 (d, $J(^{13}C\text{-}^{31}P)$ = 1.0 Hz, Ge(CH_3)$_3$). **^{31}P NMR** (202.30 MHz, CD_2Cl_2) δ = 55.0 (s). **MS** (APCI-LR) *m*/*z*: found: 463.00. [**S-1** + H]$^+$, calcd for $C_{25}H_{26}GePS$: 463.07. Elemental analysis (%): calcd for $C_{25}H_{25}GePS$ C 65.12, H 5.46, found: C 65.06, H 5.52.

*Synthesis of 1,2,5-Triphenyl-3-(trimethylgermyl)-1H-phosphole-1-selenide (**Se-1**).* A Schlenk tube was charged with DME (20 mL) and cooled to −70 °C. Then, phenylphosphane (0.11 g, 1 mmol, 1.0 equiv) was added. After that, *n*BuLi (2.5 M, 0.42 mL, 1,05 mmol, 1.05 equiv) was used for lithiation. The orange solution was stirred for 30 min and quenched with chlorotrimethylgermane (0.12 mL, 1 mmol, 1 equiv). The colorless solution was lithiated with *n*BuLi (2.5 M, 0.42 mL, 1.05 mmol, 1.05 equiv) again. After 45 min, 1,4-diphenylbuta-1,3-diyne (0.202 g, 1 mmol, 1 equiv), dissolved in DME (10 mL), was added dropwise to the orange solution. The color changed to deep blue, and after 80 min, the reaction mixture was warmed up to 40 °C and stirred for 10 min. The reaction was terminated by adding ethanol. Afterward, an excess of red selenium (237 mg, 3 mmol, 3 equiv) was added and the suspension was stirred for 16 h at rt. The crude product was purified by silica gel column chromatography with *n*-pentane/dichloromethane 1:1. The crude product was purified by silica gel column chromatography with *n*-pentane/dichloromethane 1:1. The product was obtained as an orange solid. Yield: 64% (0.326 g). **^{1}H NMR** (499.75 MHz, CD_2Cl_2) δ = 7.96−7.91 (m, 2H, 2× CH_{Ar}), 7.73−7.72 (m, 2H, 2× CH_{Ar}), 7.58 (d, $^3J(^1H\text{-}^{31}P)$ = 35.1 Hz, 1 H, $(CH_3)_3GeCCH$), 7.53−7.45 (m, 3H, 3× CH_{Ar}), 7.36−7.25 (m, 8H, 8× CH_{Ar}), 0.34 (s, 9H, 3× Ge(CH_3)). **^{13}C{^{1}H} NMR** (100.56 MHz, CD_2Cl_2) δ = 153.2 (d, $J(^{13}C\text{-}^{31}P)$ = 10.5 Hz, C_q), 150.9 (d, $J(^{13}C\text{-}^{31}P)$ = 58.7 Hz, C_q), 140.5 (d, $J(^{13}C\text{-}^{31}P)$ = 74.4 Hz, C_q), 137.8 (d, $J(^{13}C\text{-}^{31}P)$ = 29.7 Hz, CH), 134.6 (d, $J(^{13}C\text{-}^{31}P)$ = 16.2 Hz, C_q), 132.6 (s, CH), 132.5 (s, C_q), 131.5 (d, $J(^{13}C\text{-}^{31}P)$ = 11.4 Hz, CH), 130.0 (d, $J(^{13}C\text{-}^{31}P)$ = 4.0 Hz, CH), 129.5 (d, $J(^{13}C\text{-}^{31}P)$ = 12.2 Hz,

https://doi.org/10.1021/acs.organomet.3c00019
Organometallics 2023, 42, 793−802

CH), 129.5 (s, CH), 129.2 (s, CH), 128.9 (d, $J(^{13}C\text{-}^{31}P)$ = 1.9 Hz, CH), 128.3 (s, CH), 127.3 (d, $J(^{13}C\text{-}^{31}P)$ = 6.1 Hz, CH), 125.9 (d, $J(^{13}C\text{-}^{31}P)$ = 61.0 Hz, C_q), −0.4 (s, $Ge(CH_3)_3$). **^{31}P NMR** (202.30 MHz, CD_2Cl_2) δ = 43.8 (s). **^{77}Se NMR** (95.31 MHz, CD_2Cl_2) δ = −408 (d, $^1J(^{77}Se\text{-}^{31}P)$ = 743 Hz). **MS** (APCI-LR) *m/z*: found: 511.00. [**Se-1** + H]$^+$, calcd for $C_{25}H_{26}GeSeP$: 511.01. Elemental analysis (%): calcd for $C_{25}H_{25}GePSe$: C 59.10, H 4.96 found: C 59.30, H 5.05.

*Synthesis of 1-Phenyl-2,4-bis(tri-n-butylstannyl)-1H-phosphole-1-sulfide (**S-5b**).* Zirconocene dichloride (1.17 g, 4.0 mmol, 2.0 equiv) and elemental lanthanum (0.36 g, 2.6 mmol, 1.3 equiv) were transferred into a Schlenk flask. 10 mL of THF was added to the reaction vessel, followed by the addition of ethynyltri-*n*-butylstannane (3.00 g, 8.0 mmol, 4.0 equiv). The dark-colored reaction mixture was stirred for 6 h at room temperature. Then, the reaction temperature was lowered to −80 °C and dichlorophenylphosphane (0.36 g, 2.0 mmol, 1.0 equiv) was added. The reaction mixture was stirred for a further 16 h. After that, elemental sulfur (0.19 g, 6.0 mmol, 3.0 equiv) was added to the reaction vessel and stirred for a further 24 h at room temperature. The raw product was extracted with dichloromethane (3 × 30 mL) and dried over Mg_2SO_4. The solvent was removed under reduced pressure and column chromatographic purification (*n*-pentane/dichloromethane 7:3) was performed. The isolated compound was obtained as a yellow oil. Yield: 47% (0.72 g 0.97 mmol). **^{1}H NMR** (499.74 MHz, CD_2Cl_2) δ = 7.81−7.75 (m, 2H, 2× CH_{Ar}), 7.50−7.38 (m, 3H, 3× CH_{Ar}), 7.14 (d, $^3J(^1H\text{-}^{31}P)$ = 49.4 Hz, $^3J(^1H\text{-}^{119/117}Sn)$ = 36.1, $^3J(^1H\text{-}^{119/117}Sn)$ = 6.2 Hz, 1H, PCC*H*), 6.77 (d, $^2J(^1H\text{-}^{31}P)$ = 41.0 Hz, $^3J(^1H\text{-}^{119/117}Sn)$ = 36.8, 1H, PC*H*), 1.65−0.79 (m, 54H, 2× *n*-bu_3-*H*). **^{13}C{^{1}H} NMR** (100.56 MHz, CD_2Cl_2) δ = 161.0 (d, $J(^{13}C\text{-}^{31}P)$ = 10.6 Hz, C_q), 153.8 (d, $J(^{13}C\text{-}^{31}P)$ = 19.3 Hz, CH), 147.1 (d, $J(^{13}C\text{-}^{31}P)$ = 33.4 Hz, C_q), 144.9 (d, $J(^{13}C\text{-}^{31}P)$ = 54.2 Hz, CH), 132.0 (d, $J(^{13}C\text{-}^{31}P)$ = 3.2 Hz, CH), 130.9 (d, $J(^{13}C\text{-}^{31}P)$ = 11.3 Hz, CH), 129.1 (d, $J(^{13}C\text{-}^{31}P)$ = 11.9 Hz, CH), 128.0 (d, $J(^{13}C\text{-}^{31}P)$ = 69.6 Hz, C_q), 29.8 (s, *n*-Bu), 29.4 (s, *n*-Bu) 27.8 (s, *n*-Bu) 27.8 (s, *n*-Bu) 14.9 (s, *n*-Bu) 14.1 (s, *n*-Bu), 10.7 (d, $J(^{13}C\text{-}^{31}P)$ = 1.5 Hz, *n*-Bu) 10.6 (s, *n*-Bu). **^{31}P{^{1}H} NMR** (202.30 MHz, CD_2Cl_2) δ = 63.9 (s, $^2J(^{31}P\text{-}^{117}Sn)$ = 128 Hz, $^2J(^{31}P\text{-}^{119}Sn)$ = 131 Hz, $^3J(^{31}P\text{-}^{117}Sn)$ = 172 Hz, $^3J(^{31}P\text{-}^{119}Sn)$ = 176 Hz). **^{119}Sn{^{1}H} NMR** (186.25 MHz, CD_2Cl_2) δ = −38 (d, $^2J(^{31}P\text{-}^{119}Sn)$ = 134 Hz, PCC*Sn*), −46 (d, $^3J(^{31}P\text{-}^{119}Sn)$ = 169 Hz, PC*Sn*). **MS** (APCI-LR) *m/z*: 771.00 found [**S-5b** + H]$^+$, calcd for $C_{34}H_{62}PSSn_2$: 771.23; 713.07 found [**S-5b** − Bu]$^+$, calcd for $C_{30}H_{52}PSSn_2$: 713.16. Elemental analysis (%): calcd for $C_{34}H_{61}PSSn_2$ C 53.01, H 7.98, found: C 53.13, H 8.08.

*Synthesis of 1-Phenyl-2,4-bis(tri-n-butylstannyl)-1H-phosphole-1-selenide (**Se-5b**).* Zirconocene dichloride (1.17 g, 4.0 mmol, 2.0 equiv) and elemental lanthanum (0.36 g, 2.6 mmol, 1.3 equiv) were transferred into a Schlenk flask. 10 mL of THF was added to the reaction vessel, followed by the addition of ethynyltri-*n*-butylstannane (3.00 g, 8.0 mmol, 4.0 equiv). The dark-colored reaction mixture was stirred for 6 h at room temperature. Then, the reaction temperature was lowered to −80 °C and dichlorophenylphosphane (0.36 g, 2.0 mmol, 1.0 equiv) was added. The reaction mixture was stirred for a further 16 h. After that, red selenium (0.24 g, 3.0 mmol, 1.5 equiv) was added to the reaction vessel and stirred for a further 24 h at room temperature. The raw product was extracted with dichloromethane (3 × 30 mL) and dried over Mg_2SO_4. The solvent was removed under reduced pressure and column chromatographic purification (*n*-pentane/dichloromethane 4:1) was performed. The isolated compound was obtained as orange oil. Yield: 34% (0.48 g, 0.59 mmol). **^{1}H NMR** (499.74 MHz, CD_2Cl_2) δ = 7.81−7.76 (m, 2H, 2× CH_{Ar}), 7.49−7.45 (m, 1H, 1× CH_{Ar}), 7.41−7.37 (m, 2H, 2× CH_{Ar}), 7.10 (dd, $^3J(^1H\text{-}^{31}P)$ = 49.4 Hz, $^4J(^1H\text{-}^1H)$ = 0.8 Hz, $^3J(^1H\text{-}^{119/117}Sn)$ = 35.1, $^3J(^1H\text{-}^{119/117}Sn)$ = 6.6f Hz, 1H, PCC*H*), 6.85 (d, $^2J(^1H\text{-}^{31}P)$ = 42.7 Hz, $^4J(^1H\text{-}^1H)$ = 0.8 Hz, $^3J(^1H\text{-}^{119/117}Sn)$ = 35.9, 1H, PC*H*), 1.60−0.81 (m, 54H, 2× *n*-bu_3-*H*). **^{13}C{^{1}H} NMR** (100.56 MHz, CD_2Cl_2) δ = 160.8 (d, $J(^{13}C\text{-}^{31}P)$ = 9.0 Hz, C_q), 153.7 (d, $J(^{13}C\text{-}^{31}P)$ = 17.6 Hz, CH), 147.2 (d, $J(^{13}C\text{-}^{31}P)$ = 24.2 Hz, C_q), 144.9 (d, $J(^{13}C\text{-}^{31}P)$ = 45.8 Hz, CH), 132.1 (d, $J(^{13}C\text{-}^{31}P)$ = 3.0 Hz, CH), 131.5 (d, $J(^{13}C\text{-}^{31}P)$ = 11.4 Hz, CH), 129.1 (d, $J(^{13}C\text{-}^{31}P)$ = 11.9 Hz, CH), 128.2 (d, $J(^{13}C\text{-}^{31}P)$ = 61.8 Hz, C_q), 29.8 (s, *n*-Bu), 29.4 (s, *n*-Bu) 27.9 (s, *n*-Bu) 27.8 (s, *n*-Bu) 14.1 (s, *n*-Bu) 14.0 (s, *n*-Bu), 11.0 (d, $J(^{13}C\text{-}^{31}P)$ = 1.8 Hz, *n*-Bu) 10.6 (s, *n*-Bu). **^{31}P{^{1}H} NMR** (202.30 MHz, CD_2Cl_2) δ = 50.6 (s, $^2J(^{31}P\text{-}^{117}Sn)$ = 128 Hz, $^2J(^{31}P\text{-}^{119}Sn)$ = 132 Hz, $^3J(^{31}P\text{-}^{117}Sn)$ = 161 Hz, $^3J(^{31}P\text{-}^{119}Sn)$ = 169 Hz). **^{77}Se NMR** (95.31 MHz, CD_2Cl_2) δ = −478 (d, $^1J(^{77}Se\text{-}^{31}P)$ = 714 Hz). **^{119}Sn{^{1}H} NMR** (186.25 MHz, CD_2Cl_2) δ = −38 (d, $^2J(^{31}P\text{-}^{119}Sn)$ = 134 Hz, PCC*Sn*), −47 (d, $^3J(^{31}P\text{-}^{119}Sn)$ = 169 Hz, PC*Sn*). **MS** (APCI-HR) *m/z*: 819.1825 [**Se-5b** + H]$^+$, calcd for $C_{34}H_{62}PSeSn_2$: 819.1792. Elemental analysis (%): calcd for $C_{34}H_{61}PSeSn_2$ C 49.97, H 7.52, found: C 50.14, H 7.69.

*Synthesis of 1-Phenyl-2,4-bis(triphenylstannyl)-1H-phosphole (**5c**).* Zirconocene dichloride (1.17 g, 4.0 mmol, 2.0 equiv) and elemental lanthanum (0.36 g, 2.6 mmol, 1.3 equiv) were transferred into a Schlenk flask. 10 mL of THF was added to the reaction vessel, followed by the addition of ethynyltriphenylstannane (3.00 g, 8.0 mmol, 4.0 equiv). The dark-colored reaction mixture was stirred for 6 h at room temperature. Then, the reaction temperature was lowered to −80 °C and dichlorophenylphosphane (0.36 g, 2.0 mmol, 1.0 equiv) was added. The reaction mixture was stirred for a further 16 h. After that, the raw product was extracted with dichloromethane (3 × 30 mL) and dried over Mg_2SO_4. The solvent was removed under reduced pressure and a column chromatographic purification (cyclohexane/ethyl acetate 4:1) was performed (R_F = 0.6). The isolated compound was obtained as a brown oil, which was crystalized at −20 °C from a mixture of pentane and dichloromethane. The product was obtained as a colorless, crystalline solid. Yield: 74% (1.28 g 1.49 mmol). **^{1}H NMR** (399.87 MHz, CD_2Cl_2) δ = 8.04−7.10 (m, 37× CH_{Ar}). **^{13}C{^{1}H} NMR** (100.56 MHz, CD_2Cl_2) δ = 154.6 (d, $J(^{13}C\text{-}^{31}P)$ = 18.6 Hz, CH), 152.3 (d, $J(^{13}C\text{-}^{31}P)$ = 9.0 Hz, C_{Ar}), 149.2 (d, $J(^{13}C\text{-}^{31}P)$ = 6.2 Hz, C_q), 146.9 (s, C_q), 145.2 (d, $J(^{13}C\text{-}^{31}P)$ = 35.0 Hz, CH), 140.0 (s, CH), 138.6 (s, CH), 137.9−137.2 (m, CH), 136.7 (s, CH), 134.9 (d, $J(^{13}C\text{-}^{31}P)$ = 19.5 Hz, C_{Ar}), 131.1 (s, C_{Ar}), 130.2 (d, $J(^{13}C\text{-}^{31}P)$ = 1.9 Hz, C_{Ar}), 129.9−129.4 (m, C_{Ar}), 129.3−128.9 (m, C_{Ar}). **^{31}P{^{1}H} NMR** (202.30 MHz, CD_2Cl_2) δ = 35.3 (s, $^2J(^{31}P\text{-}^{117/119}Sn)$ = 70 Hz, $^3J(^{31}P\text{-}^{117}Sn)$ = 209 Hz, $^3J(^{31}P\text{-}^{119}Sn)$ = 219 Hz). **^{119}Sn{^{1}H} NMR** (186.25 MHz, CD_2Cl_2) δ = −131 (d, $^3J(^{31}P\text{-}^{119}Sn)$ = 219 Hz, PCC*Sn*), −145 (d, $^2J(^{31}P\text{-}^{119}Sn)$ = 71 Hz, PC*Sn*). **MS** (APCI-HR) *m/z*: 859.07327 [**5c** + H]$^+$, calcd for $C_{46}H_{38}PSn_2$: 859.07437. Elemental analysis (%): calcd for $C_{46}H_{37}PSn_2$: C 64.38, H 4.35 found: C 64.09, H 4.20.

*Synthesis of 1-Phenyl-2,4-bis(triphenylstannyl)-1H-phosphole-1-selenide (**Se-5c**).* Phosphole **7** (0.86 g, 1.0 mmol, 1.0 equiv) was dissolved in DCM (15 mL) at rt; red selenium (0.16 g, 2 mmol, 2 equiv) was added and stirred for 16 h. Then, the solvent was removed under reduced pressure and the raw product was purified by column chromatography (DCM; R_F = 0.4). The product was obtained as an orange crystalline solid. Yield: 41% (0.38 g 0.41 mmol). **^{1}H NMR** (499.74 MHz, CD_2Cl_2) δ = 7.60−7.17 (m, 37× CH_{Ar}). Due to overlaps in the ^{13}C NMR spectrum, just a list with the detected signals is shown. **^{13}C{^{1}H} NMR** (100.56 MHz, CD_2Cl_2) δ = 138.3, 138.0, 137.8, 137.8, 137.7, 137.6, 137.6, 137.4, 137.4, 137.3, 136.8, 136.7, 136.7, 135.2, 131.8, 131.8, 131.7, 131.4, 130.8, 130.4, 130.4, 130.3, 130.0, 129.7, 129.6, 129.4, 129.3, 129.1, 129.0, 129.0, 128.8, 128.8, 128.1. **^{31}P{^{1}H} NMR** (202.30 MHz, CD_2Cl_2) δ = 52.5 (s, $^1J(^{31}P\text{-}^{77}Se)$ = 727 Hz, $^2J(^{31}P\text{-}^{117}Sn)$ = 176 Hz, $^2J(^{31}P\text{-}^{119}Sn)$ = 184 Hz, $^3J(^{31}P\text{-}^{117}Sn)$ = 208 Hz, $^3J(^{31}P\text{-}^{119}Sn)$ = 218 Hz). **^{77}Se NMR** (95.31 MHz, CD_2Cl_2) δ = −479 (d, $^1J(^{77}Se\text{-}^{31}P)$ = 727 Hz). **^{119}Sn{^{1}H} NMR** (186.25 MHz, CD_2Cl_2) δ = −139 (d, $^2J(^{31}P\text{-}^{119}Sn)$ = 184 Hz, PC*Sn*), −148 (d, $^3J(^{31}P\text{-}^{119}Sn)$ = 218 Hz, PCC*Sn*). **MS** (APCI-HR) *m/z*: 859.071 [**Se-5c**-Se + H]$^+$, calcd for $C_{46}H_{38}PSn_2$: 859.074. Elemental analysis (%): calcd for $C_{46}H_{37}PSeSn_2$: C 58.96, H 3.98, H 4.35 found: C 58.95, H 4.22.

*Spectroscopic Data for (1E,3E)-1,4-Bis(triphenylstannyl)buta-1,3-diene (**4c**).* **^{1}H NMR** (399.87 MHz, CD_2Cl_2) δ = 7.75−7.46 (m, 13H, 13× CH_{Ar}), 7.46−7.27 (m, 19H, 19× CH_{Ar}), 6.93−6.54 (m, 2H, 2× SnCC*H*), **^{13}C{^{1}H} NMR** (100.56 MHz, CD_2Cl_2) δ = 137.3 (s, $J(^{13}C\text{-}^{117/119}Sn)$ = 8.2 Hz, $J(^{13}C\text{-}^{117/119}Sn)$ = 41.0 Hz, C_q), 136.9.3 (s, $J(^{13}C\text{-}^{117/119}Sn)$ = 37.7 Hz, CH), 129.0 (s, $J(^{13}C\text{-}^{117/119}Sn)$ = 11.4 Hz, CH), 128.8 (s, $J(^{13}C\text{-}^{117/119}Sn)$ = 11.2 Hz, CH), 128.7 (s, CH), 128.5 (s, CH). **^{119}Sn{^{1}H} NMR** (186.25 MHz, CD_2Cl_2) δ = −143 (s). **MS** (APCI) *m/z*: 351.02 [Ph_3Sn + H]$^+$, calcd for: 351.02. **4c** was

https://doi.org/10.1021/acs.organomet.3c00019
Organometallics 2023, 42, 793−802

obtained in the synthesis of **5c** or **Se-5c**, after attempted chromatographic purification, *via* fractional crystallization from the eluate, evaporated to dryness, and redissolved in dichloromethane, adding an equal volume of pentane, followed by crystallization at −20 °C. **5c** or **Se-5c** crystallize first, followed by a second crop consisting of **4c**.

■ ASSOCIATED CONTENT

Supporting Information

The Supporting Information is available free of charge at https://pubs.acs.org/doi/10.1021/acs.organomet.3c00019.

Crystallographic details, computational details, and NMR and MS spectra (PDF)

Detailed molecule coordinates of all optimized structures (TXT)

Accession Codes

CCDC 2223036−2223041 contain the supplementary crystallographic data for this paper. These data can be obtained free of charge via www.ccdc.cam.ac.uk/data_request/cif, or by emailing data_request@ccdc.cam.ac.uk, or by contacting The Cambridge Crystallographic Data Centre, 12 Union Road, Cambridge CB2 1EZ, UK; fax: +44 1223 336033.

■ AUTHOR INFORMATION

Corresponding Authors

Zsolt Kelemen − *Department of Inorganic and Analytical Chemistry, Budapest University of Technology and Economics, H-1111 Budapest, Hungary;* orcid.org/0000-0002-4787-9804; Email: kelemen.zsolt@vbk.bme.hu

Rudolf Pietschnig − *Institute for Chemistry and CINSaT, University of Kassel, 34132 Kassel, Germany;* orcid.org/0000-0003-0551-3633; Email: pietschnig@uni-kassel.de

Authors

Fabian Roesler − *Institute for Chemistry and CINSaT, University of Kassel, 34132 Kassel, Germany*

Máté Kovács − *Department of Inorganic and Analytical Chemistry, Budapest University of Technology and Economics, H-1111 Budapest, Hungary;* orcid.org/0000-0003-2820-207X

Clemens Bruhn − *Institute for Chemistry and CINSaT, University of Kassel, 34132 Kassel, Germany*

Complete contact information is available at: https://pubs.acs.org/10.1021/acs.organomet.3c00019

Author Contributions

F.R. carried out the experimental work and M.K. performed the computational work. The crystallographic work was carried out by C.B. R.P. and Z.K. wrote the manuscript. The SI was compiled by all authors.

Notes

The authors declare no competing financial interest.

■ ACKNOWLEDGMENTS

The authors would like to thank the German Science Fund (DFG) for financial support (Project PI 353/11-1 and CRC 1319). Z.K. is grateful for the general support of the János Bolyai Research Scholarship and Project UNKP-22-5-BME-298. The authors are grateful to Dennis Langgut for additional analytical measurements.

■ REFERENCES

(1) Romero-Nieto, C.; López-Andarias, A.; Egler-Lucas, C.; Gebert, F.; Neus, J.-P.; Pilgram, O. Paving the Way to Novel Phosphorus-Based Architectures: A Noncatalyzed Protocol to Access Six-Membered Heterocycles. *Angew. Chem. Int. Ed.* **2015**, *54*, 15872−15875.

(2) Bouit, P.-A.; Escande, A.; Szűcs, R.; Szieberth, D.; Lescop, C.; Nyulászi, L.; Hissler, M.; Réau, R. Dibenzophosphapentaphenes: exploiting P chemistry for gap fine-tuning and coordination-driven assembly of planar polycyclic aromatic hydrocarbons. *J. Am. Chem. Soc.* **2012**, *134*, 6524−6527.

(3) Delouche, T.; Mocanu, A.; Roisnel, T.; Szűcs, R.; Jacques, E.; Benkő, Z.; Nyulászi, L.; Bouit, P.-A.; Hissler, M. π-Extended Phosphepines: Redox and Optically Active P-Heterocycles with Nonplanar Framework. *Org. Lett.* **2019**, *21*, 802−806.

(4) Fukazawa, A.; Hara, M.; Okamoto, T.; Son, E.-C.; Xu, C.; Tamao, K.; Yamaguchi, S. Bis-phosphoryl-bridged stilbenes synthesized by an intramolecular cascade cyclization. *Org. Lett.* **2008**, *10*, 913−916.

(5) Reus, C.; Stolar, M.; Vanderkley, J.; Nebauer, J.; Baumgartner, T. A Convenient N-Arylation Route for Electron-Deficient Pyridines: The Case of π-Extended Electrochromic Phosphaviologens. *J. Am. Chem. Soc.* **2015**, *137*, 11710−11717.

(6) Washington, M. P.; Gudimetla, V. B.; Laughlin, F. L.; Deligonul, N.; He, S.; Payton, J. L.; Simpson, M. C.; Protasiewicz, J. D. Phosphorus can also be a "photocopy". *J. Am. Chem. Soc.* **2010**, *132*, 4566−4567.

(7) Wu, S.; Rheingold, A. L.; Golen, J. A.; Grimm, A. B.; Protasiewicz, J. D. Synthesis of a Luminescent Azaphosphole. *Eur. J. Inorg. Chem.* **2016**, *2016*, 768−773.

(8) Wittig, G.; Geissler, G. Zur Reaktionsweise des Pentaphenylphosphors und einiger Derivate. *Justus Liebigs Ann. Chem.* **1953**, *580*, 44−57.

(9) Klintuch, D.; Höfler, M. V.; Wissel, T.; Bruhn, C.; Gutmann, T.; Pietschnig, R. Trifunctional Silyl Groups as Anchoring Units in the Preparation of Luminescent Phosphole−Silica Hybrids. *Inorg. Chem.* **2021**, *60*, 14263−14274.

(10) Duffy, M. P.; Delaunay, W.; Bouit, P.-A.; Hissler, M. π-Conjugated phospholes and their incorporation into devices: components with a great deal of potential. *Chem. Soc. Rev.* **2016**, *45*, 5296−5310.

(11) Fave, C.; Cho, T.-Y.; Hissler, M.; Chen, C.-W.; Luh, T.-Y.; Wu, C.-C.; Réau, R. First Examples of Organophosphorus-Containing Materials for Light-Emitting Diodes. *J. Am. Chem. Soc.* **2003**, *125*, 9254−9255.

(12) Joly, D.; Bouit, P.-A.; Hissler, M. Organophosphorus derivatives for electronic devices. *J. Mater. Chem. C* **2016**, *4*, 3686−3698.

(13) Roesler, F.; Kaban, B.; Klintuch, D.; Ha, U.-M.; Bruhn, C.; Hillmer, H.; Pietschnig, R. Tailoring Phospholes for Imprint of Fluorescent 3D Structures. *Eur. J. Inorg. Chem.* **2019**, *2019*, 4820−4825.

(14) Mathey, F. The organic chemistry of phospholes. *Chem. Rev.* **1988**, *88*, 429−453.

(15) Tokura, Y.; Xu, S.; Kojima, Y.; Miura, M.; Hirano, K. Pd-catalysed, Ag-assisted C2−H alkenylation of benzophospholes. *Chem. Commun.* **2022**, *58*, 12208−12211.

(16) Märkl, G.; Potthast, R. A Simple Synthesis of Phospholes. *Angew. Chem. Int. Ed.* **1967**, *6*, No. 86.

(17) Klintuch, D.; Krekić, K.; Bruhn, C.; Benkő, Z.; Pietschnig, R. A Rational Synthetic Approach to 2,5-Diphenyl-β-silyl Phospholes. *Eur. J. Inorg. Chem.* **2016**, *2016*, 718−725.

(18) Klintuch, D.; Kirchmeier, A.; Bruhn, C.; Pietschnig, R. Synthetic access and luminescence tuning in a series of β-H and β-silyl substituted phospholes. *Dyes Pigm.* **2020**, *180*, No. 108443.

(19) Roesler, F.; Kovács, M.; Bruhn, C.; Kelemen, Z.; Pietschnig, R. Phosphetes via transition metal free ring closure - taking the proper turn at a thermodynamic crossing. *Chem. - Eur. J.* **2021**, *27*, 9782−9790.

(20) Forissier, K.; Ricard, L.; Carmichael, D.; Mathey, F. 2,5-Di-(*tert*-butyl)phospholyl sandwich complexes containing group 14 elements (Ge, Sn, Pb). Synthesis, molecular structure, and ring transfer chemistry of $[M(PC_4H_2Bu^t_2)_2]$ (M = Sn, Pb). *Chem. Commun.* **1999**, 1273−1274.
(21) Matano, Y.; Hayashi, Y.; Suda, K.; Kimura, Y.; Imahori, H. Synthesis of 2-alkenyl- and 2-alkynyl-benzo[*b*]phospholes by using palladium-catalyzed cross-coupling reactions. *Org. Lett.* **2013**, *15*, 4458−4461.
(22) Saito, A.; Matano, Y.; Imahori, H. Synthesis of α,α'-linked oligophospholes and polyphospholes by using Pd-CuI-promoted Stille-type coupling. *Org. Lett.* **2010**, *12*, 2675−2677.
(23) Kaithal, A.; Sasmal, H. S.; Dutta, S.; Schäfer, F.; Schlichter, L.; Glorius, F. cis-Selective Hydrogenation of Aryl Germanes: A Direct Approach to Access Saturated Carbo- and Heterocyclic Germanes. *J. Am. Chem. Soc.* **2023**, *145*, 4109−4118.
(24) Krenske, E. H. Reductions of phosphine oxides and sulfides by perchlorosilanes: evidence for the involvement of donor-stabilized dichlorosilylene. *J. Org. Chem.* **2012**, *77*, 1−4.
(25) Naumann, K.; Zon, G.; Mislow, K. Use of hexachlorodisilane as a reducing agent. Stereospecific deoxygenation of acyclic phosphine oxides. *J. Am. Chem. Soc.* **1969**, *91*, 7012−7023.
(26) Zon, G.; DeBruin, K. E.; Naumann, K.; Mislow, K. Stereospecific desulfurization of acyclic phosphine sulfides with hexachlorodisilane and the alkaline hydrolysis of monoalkoxy- and monoalkylthiophosphonium salts. *J. Am. Chem. Soc.* **1969**, *91*, 7023−7027.
(27) Griffiths, D. V.; Groombridge, H. J.; Mahoney, P. M.; Swetnam, S. P.; Walton, G.; York, D. C. Nucleophilic addition to dimethylvinylphosphine sulfide as a convenient route to polydentate ligands containing the 2-dimethylphosphinoethyl unit. *Tetrahedron* **2005**, *61*, 4595−4600.
(28) Fagan, P. J.; Nugent, W. A. Synthesis of main group heterocycles by metallacycle transfer from zirconium. *J. Am. Chem. Soc.* **1988**, *110*, 2310−2312.
(29) Bousrez, G.; Nicolas, E.; Martinez, A.; Chevreux, S.; Jaroschik, F. [4+2] versus [2+2] Homodimerization in P(V) Derivatives of 2,4-Disubstituted Phospholes. *Heteroat. Chem.* **2019**, *2019*, 1−10.
(30) Bousrez, G.; Jaroschik, F.; Martinez, A.; Harakat, D.; Nicolas, E.; Le Goff, X. F.; Szymoniak, J. Reactivity differences between 2,4- and 2,5-disubstituted zirconacyclopentadienes: a highly selective and general approach to 2,4-disubstituted phospholes. *Dalton Trans.* **2013**, *42*, 10997−11004.
(31) Bondi, A. van der Waals Volumes and Radii. *J. Phys. Chem. A* **1964**, *68*, 441−451.
(32) Hong, Y.; Lam, J. W. Y.; Tang, B. Z. Aggregation-induced emission. *Chem. Soc. Rev.* **2011**, *40*, 5361−5388.
(33) Wu, Q.; Zhang, T.; Peng, Q.; Wang, D.; Shuai, Z. Aggregation induced blue-shifted emission − the molecular picture from a QM/MM study. *Phys. Chem. Chem. Phys.* **2014**, *16*, 5545−5552.
(34) Gierschner, J.; Park, S. Y. Luminescent distyrylbenzenes: tailoring molecular structure and crystalline morphology. *J. Mater. Chem. C* **2013**, *1*, 5818−5832.
(35) Oelkrug, D.; Tompert, A.; Egelhaaf, H.-J.; Hanack, M.; Steinhuber, E.; Hohloch, M.; Meier, H.; Stalmach, U. Towards highly luminescent phenylene vinylene films. *Synth. Met.* **1996**, *83*, 231−237.
(36) Huang, Y.-S.; Gierschner, J.; Schmidtke, J. P.; Friend, R. H.; Beljonne, D. Tuning interchain and intrachain interactions in polyfluorene copolymers. *Phys. Rev. B* **2011**, *84*, No. 205311.
(37) Dong, Y.; Xu, B.; Zhang, J.; Tan, X.; Wang, L.; Chen, J.; Lv, H.; Wen, S.; Li, B.; Ye, L.; Zou, B.; Tian, W. Piezochromic Luminescence Based on the Molecular Aggregation of 9,10-Bis((E)-2-(pyrid-2-yl)vinyl)anthracene. *Angew. Chem. Int. Ed.* **2012**, *51*, 10782−10785.
(38) An, B.-K.; Kwon, S.-K.; Jung, S.-D.; Park, S. Y. Enhanced Emission and Its Switching in Fluorescent Organic Nanoparticles. *J. Am. Chem. Soc.* **2002**, *124*, 14410−14415.
(39) Kumaravel, M.; Joel, T. M.; Maravanji, S. B. Chalcogenide derivatives of 1,2,5-triphenyl-1H-phosphole: structure and photophysical properties. *Tetrahedron Lett.* **2014**, *55*, 2957−2961.
(40) Nagel, U.; Bublewitz, A. Enantioselektive Katalyse, VIII. Neue 1,2-Bisphosphanliganden mit vier stereogenen Zentren und zusätzlichen Methoxygruppen für die asymmetrische katalytische Hydrierung. *Chem. Ber.* **1992**, *125*, 1061−1072.
(41) Hay, A. S. Oxidative Coupling of Acetylenes. II[1]. *J. Org. Chem.* **1962**, *27*, 3320−3321.
(42) Sheldrick, G. M. Crystal structure refinement with SHELXL. *Acta Crystallogr., Sect. C: Struct. Chem.* **2015**, *71*, 3−8.
(43) Dolomanov, O. V.; Bourhis, L. J.; Gildea, R. J.; Howard, J. A. K.; Puschmann, H. OLEX2: a complete structure solution, refinement and analysis program. *J. Appl. Crystallogr.* **2009**, *42*, 339−341.
(44) Macrae, C. F.; Sovago, I.; Cottrell, S. J.; Galek, P. T. A.; McCabe, P.; Pidcock, E.; Platings, M.; Shields, G. P.; Stevens, J. S.; Towler, M.; Wood, P. A. Mercury 4.0: from visualization to analysis, design and prediction. *J. Appl. Crystallogr.* **2020**, *53*, 226−235.

https://doi.org/10.1021/acs.organomet.3c00019
Organometallics 2023, 42, 793−802